CellPress
OPEN ACCESS

Trends in
Biotechnology

Resource Article

Streamlined and efficient genome editing in *Cupriavidus necator* H16 using an optimised SIBR-Cas system

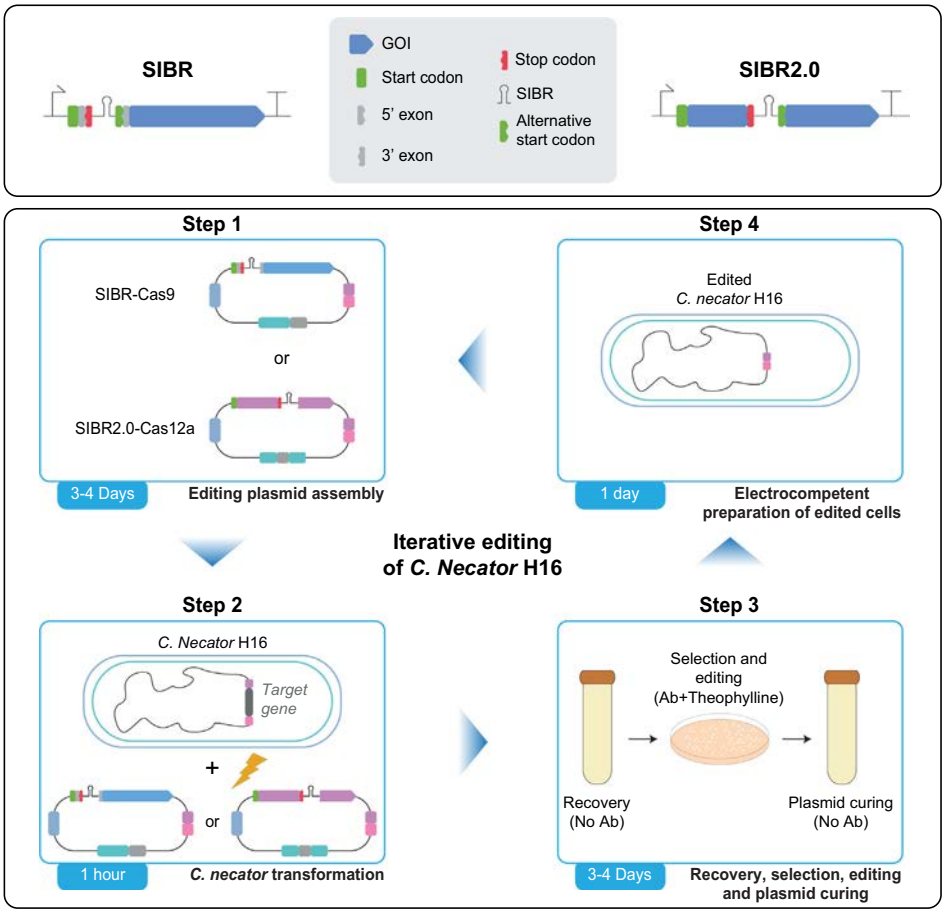

This study developed two simple, efficient, and rapid genome editing tools termed Self-splicing Intron-Based Riboswitch-Cas9 (SIBR-Cas9) and SIBR2.0-Cas12a, for editing the genome of the industrially relevant microbial strain *Cupriavidus necator* H16. SIBR2.0 can additionally be used to control the expression of virtually any gene in mesophilic prokaryotes.

Simona Della Valle, Enrico Orsi, Sjoerd C.A. Creutzburg, Luc F.M. Jansen, Evangelia-Niki Pentari, Chase L. Beisel, Harrison Steel, Pablo I. Nikel, Raymond H.J. Staals, Nico J. Claassens, John van der Oost, Wei E. Huang, Constantinos Patinios

wei.huang@eng.ox.ac.uk (W.E. Huang)
constantinos.patinios@gmc.vu.lt (C. Patinios).

Highlights

The original Self-splicing Intron-Based Riboswitch (SIBR) was used successfully to control the expression of Cas9 in *Cupriavidus necator*, yielding >80% editing efficiency within 48 h after electroporation.

SIBR was not sufficient to control the expression of Cas12a, leading to the discovery of an alternative translation initiation site within the original SIBR.

SIBR2.0 was developed to allow the integration of SIBR within the coding sequence of any gene of interest, splitting the gene in two distinctive exons and avoiding alternative translation of functional proteins.

SIBR2.0 was used successfully to control the expression of Cas12a in *C. necator*, resulting in ~70% editing efficiency within 48 h after electroporation.

Iterative genome editing of *C. necator* can be achieved within ~4 days, accelerating the use of this microorganism in biotechnological processes.

Trends in Biotechnology, June 2025, Vol. 43, No. 6
https://doi.org/10.1016/j.tibtech.2025.02.006

© 2025 The Authors. Published by Elsevier Ltd. This is an open access article under the CC BY license (http://creativecommons.org/licenses/by/4.0/).

Check for updates

Trends in Biotechnology

CellPress OPEN ACCESS

Resource Article

Streamlined and efficient genome editing in *Cupriavidus necator* H16 using an optimised SIBR-Cas system

Simona Della Valle[1,7], Enrico Orsi[2,7], Sjoerd C.A. Creutzburg[3], Luc F.M. Jansen[2], Evangelia-Niki Pentari[2], Chase L. Beisel[4,5], Harrison Steel[1], Pablo I. Nikel[2], Raymond H.J. Staals[3], Nico J. Claassens[3], John van der Oost[3], Wei E. Huang[1,*], and Constantinos Patinios[3,4,6,8,*]

***Cupriavidus necator* H16 is a promising microbial platform strain for CO_2 valorisation. While *C. necator* is amenable to genome editing, existing tools are often inefficient or rely on lengthy protocols, hindering its rapid transition to industrial applications. In this study, we simplified and accelerated the genome editing pipeline for *C. necator* by harnessing the Self-splicing Intron-Based Riboswitch (SIBR) system. We used SIBR to tightly control and delay Cas9-based counterselection, achieving >80% editing efficiency at two genomic loci within 48 h after electroporation. To further increase the versatility of the genome editing toolbox, we upgraded SIBR to SIBR2.0 and used it to regulate the expression of Cas12a. SIBR2.0-Cas12a could mediate gene deletion in *C. necator* with ~70% editing efficiency. Overall, we streamlined the genome editing pipeline for *C. necator*, facilitating its potential role in the transition to a bio-based economy.**

Introduction

To promote the transition from a fossil-based to a bio-based economy, microorganisms which can grow on CO_2 or CO_2 derivatives are increasingly studied [1–4]. In particular, the β-proteobacterium *C. necator* H16 (formerly known as *Ralstonia eutropha* H16) has emerged as a promising microorganism due to its ability to convert CO_2 into value-added compounds [5]. *C. necator* can naturally grow on CO_2 and hydrogen via the Calvin–Benson–Bassham cycle, and can also utilise formate derived from electrochemical CO_2 reduction as the sole carbon source [6]. These features make *C. necator* an ideal microorganism for biotechnological processes that aim towards **CO_2 valorisation** (see Glossary).

Despite these promising properties, the potential of *C. necator* as a biotechnological platform strain remains untapped, which is partly attributed to the lack of efficient, simple, and rapid genome editing tools [7]. To date, one of the most common practices for gene deletion or insertion relies on the use of a suicide-vector system that includes two crossover events [7]. The first crossover event selects for the integration of the suicide vector in the genome of *C. necator* through an antibiotic marker, whereas the second crossover event is mediated by a counterselection cassette encoding *sacB* or *cre/loxP* [7–9]. Alternative approaches use the Tn*5* transposon, which randomly integrates into the bacterial chromosome, mediating gene knockouts or knock-ins [10–12]. Another approach involves the RalsTron system, developed as an alternative to random intron integration [13]. More recently, an inducible **CRISPR-Cas9** system was used for genome editing of *C. necator* [14]. Although the authors report high editing efficiencies, the editing protocol is prolonged (over a week). A faster CRISPR-based genome editing tool was also developed

Technology readiness

The Self-splicing Intron-Based Riboswitch (SIBR) and SIBR2.0 technologies developed in this study are currently at a Technological Readiness Level (TRL) of 4, indicating their validation in laboratory settings using the *Cupriavidus necator ΔH16_A0006ΔphaC* and *Escherichia coli* DH10B microbial strains. Although our technologies show robustness across different genes and microorganisms, there are still several challenges that must be addressed before their transition to higher TRLs. These challenges include the high toxicity of the theophylline inducer, the low number of resulting colonies using SIBR-Cas9 or SIBR2.0-Cas12a, the observed low number of resulting protein molecules after the splicing of SIBR (important when SIBR is used for applications where high protein production is required), and the restricted experimentation to mesophilic bacteria. To overcome these challenges, future advancements should focus on expanding the range of aptamers, inducers, and introns used for SIBRs, extend to organisms outside the domain of bacteria, extend to organisms outside the mesophilic range, and investigate how to increase recombination efficiency and protein production. Moreover, to implement SIBR in an organism, transformation protocols and replicative plasmids should already be established. When these readiness criteria are met, SIBR and SIBR2.0 will constitute a robust system to control the expression of virtually any protein of interest, in any organism of interest, facilitating the advancement of biotechnological processes from lab to industrial scale.

© 2025 The Authors. Published by Elsevier Ltd. This is an open access article under the CC BY license (http://creativecommons.org/licenses/by/4.0/).

but resulted in low editing efficiencies [15]. Therefore, an efficient, standardised, and rapid genome editing tool is still required for the full exploitation of *C. necator*.

Recently, the **SIBR** system was developed and applied to tightly control the expression of **Cas12a** at the translational level [16]. This system allows the endogenous **homologous recombination (HR)** machinery to perform allelic exchanges before inducing **CRISPR-Cas-mediated counterselection**, resulting in efficient gene deletion (between 40% and 100%) in phylogenetically diverse bacterial species such as *Escherichia coli*, *Pseudomonas putida*, *Flavobacterium* IR1, and *Clostridium autoethanogenum* [16,17]. This genetic control framework is designed to be gene- and organism-independent and does not require the use of inducible promoters or the expression of any additional heterologous transcription factors or enzymes, making it ideal for non-model bacterial species. Moreover, a key feature of SIBR-Cas is that it enables distinct temporal separation of HR and CRISPR-Cas counterselection, which is crucial for successful editing, particularly in bacterial species with inefficient endogenous HR system or when exogenous recombinases (e.g., λ Red) are not characterised and used in that species.

In this work, we used the previously established SIBR system to tightly and inducibly control the expression of Cas9 in *C. necator*, achieving ~80% editing efficiency at two genomic loci (*glcEF* and *acoC*), within just 48 h after electroporation. Then, to expand the genome editing toolbox for *C. necator*, we tested the original SIBR design to control the expression of Cas12a. This attempt was initially unsuccessful due to an alternative translation initiation site within the original SIBR, which was organism- and gene-dependent. To address this limitation, we developed an updated version of SIBR, named SIBR2.0. Unlike SIBR, SIBR2.0 can be introduced along the coding sequence (CDS) of the gene of interest (GOI), splitting a gene into two distinct **exon** sequences. This design ensures that, even in the presence of an alternative translation initiation site, only non-functional proteins will be expressed. We first validated SIBR2.0 by controlling the expression of the T7 RNA polymerase (T7 RNAP) in *E. coli*. We then used SIBR2.0 to tightly and inducibly control the expression of Cas12a in *C. necator*. Last, using SIBR2.0 we successfully enabled CRISPR-Cas12a-mediated genome editing in *C. necator* with ~70% editing efficiency.

Results

SIBR can tightly and inducibly control the expression of Cas9 in *C. necator*

SIBR was previously used to tightly control and inducibly express Cas12a (SIBR-Cas12a) in *E. coli*, *P. putida*, *Flavobacterium* IR1, and *C. autoethanogenum* [16,17]. Since Cas12a has not been successfully used in *C. necator* before, we initially opted to utilise Cas9 as it has been shown to be functional in this bacterium [14,15]. To develop SIBR-Cas9 in *C. necator*, we followed a series of four checkpoint controls.

First, we verified the functionality of P_{lacUV5} by expressing mRFP in *C. necator* (Figure S1 in the supplemental information online) as this promoter was used to express SIBR-Cas12a and the CRISPR (cr)RNA in the original SIBR-Cas setup [16].

Second, we tested the effect of theophylline on the growth of *C. necator*. Theophylline is the inducer for the splicing of SIBR and, to the best of our knowledge, its toxicity has never been tested in this organism. We performed a toxicity assay to determine the optimal theophylline concentration that will allow for the splicing of SIBR whilst ensuring the viability of the bacterium. The assay demonstrated that theophylline concentrations above 5 mM compromise growth, with a 30% decrease in growth rate at 10 mM and up to a 70% decrease when the concentration is increased to 20 mM (Figure S2 in the supplemental information online). Based on these results, we used 5 mM theophylline as the working concentration of the inducer for all subsequent experiments.

[1]Department of Engineering Science, University of Oxford, Oxford, UK
[2]The Novo Nordisk Foundation Centre for Biosustainability, Technical University of Denmark, Lyngby, Denmark
[3]Laboratory of Microbiology, Wageningen University and Research, Wageningen, The Netherlands
[4]Helmholtz Institute for RNA-based Infection Research (HIRI), Helmholtz Centre for Infection Research (HZI), Würzburg, Germany
[5]Medical Faculty, University of Würzburg, Würzburg, Germany
[6]LSC-EMBL Partnership Institute for Genome Editing Technologies, Life Sciences Center, Vilnius University, Vilnius, Lithuania
[7]These authors contributed equally
[8]Lead contact

*Correspondence:
wei.huang@eng.ox.ac.uk (W.E. Huang) and
constantinos.patinios@gmc.vu.lt (C. Patinios).

Third, we assessed the functionality of Cas9 through the traditional targeting and cell killing assay, by constitutively expressing Cas9 and the single guide (sg)RNA under P_{lacUV5} (Figure 1A). To mediate targeting, we designed two sgRNAs targeting the *glcF* locus (T1 and T2, see Table S2 in the supplemental information online). We chose *glcF* as the target gene as it has been previously inactivated in *C. necator* [18]. For control, we designed a nontargeting (NT) sgRNA that did not target any genomic sequence in *C. necator*. Subsequently, we electroporated the Cas9-sgRNA constructs into *C. necator* and determined the colony counts using a newly developed protocol for electrocompetent cell preparation (Figure 1B and see STAR★METHODS). For both T1 and T2 sgRNAs, we observed a ~10^4-fold reduction in the colony counts compared with the NT sgRNA control (Figure 1C), confirming the functionality of our CRISPR-Cas9 system in *C. necator*. Since T1 sgRNA showed the most drastic reduction in colony counts, we used it for subsequent experiments.

Fourth, we assessed the inducibility of the SIBR system in *C. necator*. To do this, we introduced SIBR variants with increased splicing efficiency (Int2<Int3<Int4; lowest to highest splicing efficiency) [16] directly after the start codon of the *cas9* gene (Figure 1A) and combined them with the constitutively expressed *glcF*-T1 sgRNA. Then, we tested for inducible targeting and cell killing by transforming and subjecting *C. necator* cells on media containing or omitting the theophylline inducer (Figure 1D). Transformants subjected to noninducing conditions yielded ~10^5 colony counts, irrespective of the SIBR variant used. Using SIBR-Int2-Cas9 did not result in colony count reduction, even in the presence of theophylline. This result was expected since SIBR-Int2 was previously shown to have low splicing activity, resulting in little or no protein production after induction [16]. By contrast, cells transformed with SIBR-Int3-Cas9 or SIBR-Int4-Cas9 and plated on media containing theophylline, had a ~10^5-fold reduction in total colony counts (Figure 1E).

To further assess the robustness of SIBR in *C. necator*, we selected SIBR-Int4-Cas9 and targeted another gene, *acoC*, which encodes the E2 subunit of a branched-chain alpha-keto acid dehydrogenase. The products of *acoC* and its enclosing *acoXABC* operon are involved in the catabolism of acetoin in *C. necator* [19,20]. Genes within this locus are not essential and have been previously deleted as part of metabolic engineering efforts [21,22], making them a suitable target for our assays. By using any of three sgRNAs targeting the *acoC* locus (T1, T2, and T3, Table S2), we showed that a reduction in total colony counts was possible only when the transformed cells were subjected to inducing conditions (Figure S3 in the supplemental information online). As *acoC*-T2 sgRNA exhibited the most drastic counterselection activity from all three tested sgRNAs, it was selected for subsequent targeting of this genomic locus.

SIBR-Cas9 mediates efficient genome editing in *C. necator*

After confirming stringent and inducible expression of Cas9 using SIBR-Int4 in *C. necator*, we proceeded by testing the effect of SIBR-Int4-Cas9 for editing its genome. To obtain the knockout of the *glcEF* genes (resulting in the deletion of two glycolate dehydrogenase subunits), we cloned homology arms (HArms) corresponding to the upstream and downstream of the target locus. Then, we introduced them into plasmids bearing either the constitutively expressed Cas9 or the SIBR-Int4-Cas9, including either of the *glcF*-T1 sgRNA or the NT sgRNA control. Resulting colonies with or without SIBR induction were counted (Figure S4 in the supplemental information online) and screened for the desired edit (Figure 1F and Figure S5 in the supplemental information online).

The NT sgRNA controls resulted in low (<5%) editing efficiency for all combinations tested (Figure 1G), indicating the possibility of (infrequent) HR between the genome of *C. necator*

Glossary

Cas12a: an RNA-guided endonuclease that differs from Cas9 for its T-rich PAM sequence (5′-TTTV-3′), guide RNA structure, and cleavage mechanism (staggered cuts with 5′ overhangs).
CO_2 valorisation: in biotechnology, this refers to the process of utilising carbon dioxide (or its derivatives) as a feedstock to produce valuable organic compounds and materials, such as chemicals or biopolymers, through biological means, for example, by using microorganisms as cell factories.
CRISPR-Cas9: a groundbreaking gene editing technology that enables precise modifications of DNA by using a guide RNA to direct the Cas9 enzyme to cut specific DNA sequences, allowing for targeted genetic alterations. Cas9 is a single endonuclease that recognizes a G-rich PAM with the sequence 5′-NGG-3′ and performs blunt-ended double-stranded DNA breaks.
CRISPR-Cas-mediated counterselection: a genome editing process that uses the CRISPR-Cas system (guide RNA and Cas protein) to selectively target and cleave unmodified target sequences, resulting in the elimination of unmodified cells and the survival of cells with the desired modification(s). This process enhances the selection of correctly edited cells by eliminating the nonedited ones.
Exon: a segment of a gene that remains in the mature RNA molecule after RNA splicing.
Homologous recombination (HR): a genetic process that involves the exchange of genetic material between similar or identical DNA sequences, facilitating horizontal gene transfer, genetic diversity, and accurate DNA repair during DNA damage or during genome editing.
Self-splicing Intron-Based Riboswitch (SIBR): a regulatory RNA element that combines a self-splicing intron with a ligand-binding aptamer, allowing for tight and inducible control over gene expression in bacteria through splicing modulation in response to specific molecules.

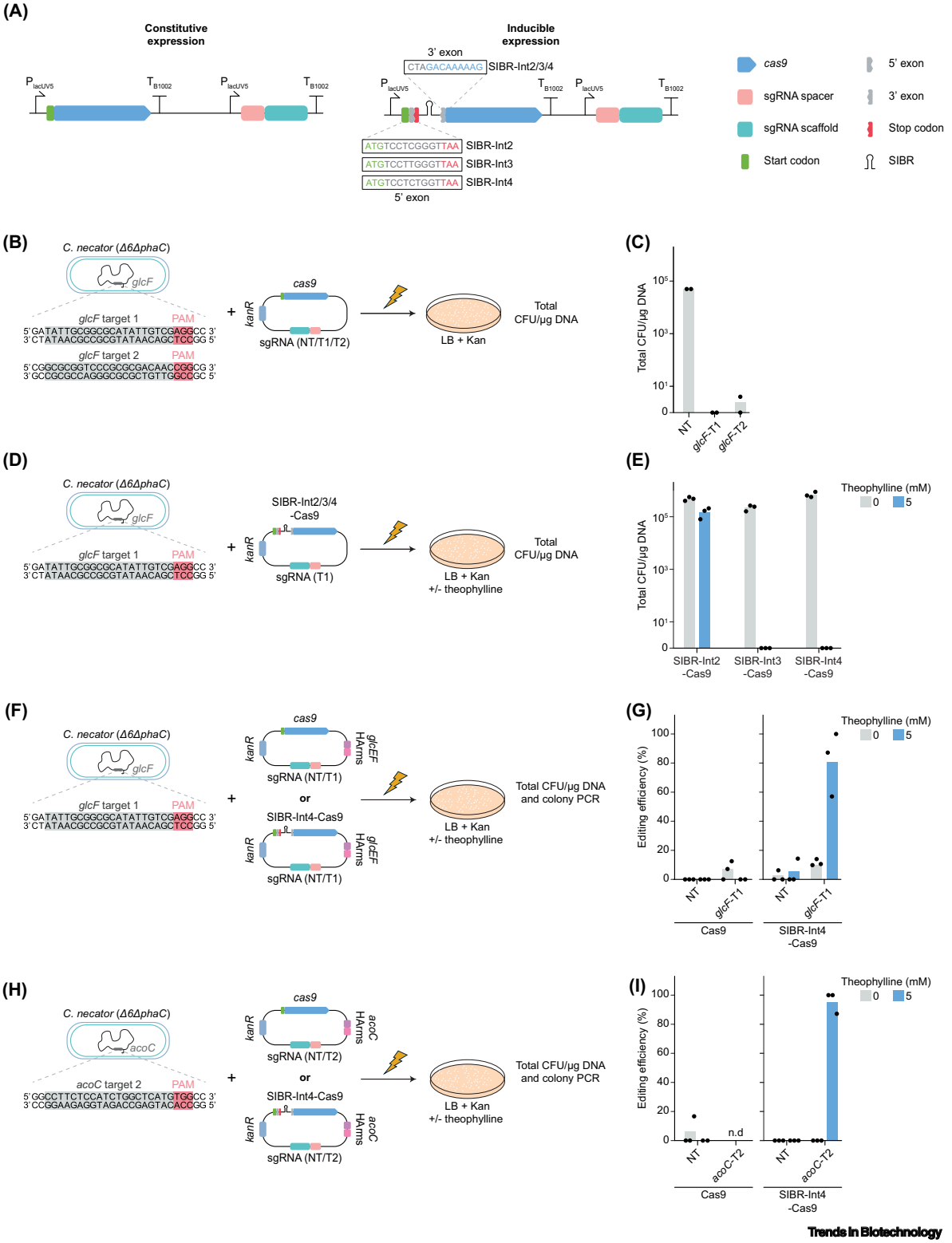
(A)
Constitutive expression
Inducible expression
3' exon
CTAGACAAAAAG SIBR-Int2/3/4
ATGTCCTCGGGTTAA SIBR-Int2
ATGTCCTTGGGTTAA SIBR-Int3
ATGTCCTCTGGTTAA SIBR-Int4
5' exon
cas9
sgRNA spacer
sgRNA scaffold
Start codon
5' exon
3' exon
Stop codon
SIBR
(B)
C. necator (Δ6ΔphaC)
glcF
glcF target 1 PAM
5' GATATTGCGGCGCATATTGTCGAGGCC 3'
3' CTATAACGCCGCGTATAACAGCTCCGG 5'
glcF target 2 PAM
5' CGGCGCGGTCCCGCGCGACAACCGGCG 3'
3' GCCGCGCCAGGGCGCGCTGTTGGCGC 5'
cas9
kanR
sgRNA (NT/T1/T2)
LB + Kan
Total CFU/μg DNA
(C)
Total CFU/μg DNA
NT
glcF-T1
glcF-T2
(D)
C. necator (Δ6ΔphaC)
glcF
glcF target 1 PAM
5' GATATTGCGGCGCATATTGTCGAGGCC 3'
3' CTATAACGCCGCGTATAACAGCTCCGG 5'
SIBR-Int2/3/4 -Cas9
kanR
sgRNA (T1)
LB + Kan
+/- theophylline
Total CFU/μg DNA
(E)
Theophylline (mM)
0
5
Total CFU/μg DNA
SIBR-Int2 -Cas9
SIBR-Int3 -Cas9
SIBR-Int4 -Cas9
(F)
C. necator (Δ6ΔphaC)
glcF
glcF target 1 PAM
5' GATATTGCGGCGCATATTGTCGAGGCC 3'
3' CTATAACGCCGCGTATAACAGCTCCGG 5'
cas9
kanR
glcEF HArms
sgRNA (NT/T1)
or
SIBR-Int4-Cas9
sgRNA (NT/T1)
LB + Kan
+/- theophylline
Total CFU/μg DNA and colony PCR
(G)
Theophylline (mM)
0
5
Editing efficiency (%)
NT
glcF-T1
Cas9
SIBR-Int4 -Cas9
(H)
C. necator (Δ6ΔphaC)
acoC
acoC target 2 PAM
5' GGCCTTCTCCATCTGGCTCATGTGGCC 3'
3' CCGGAAGAGGTAGACCGAGTACACCGG 5'
cas9
kanR
acoC HArms
sgRNA (NT/T2)
or
SIBR-Int4-Cas9
sgRNA (NT/T2)
LB + Kan
+/- theophylline
Total CFU/μg DNA and colony PCR
(I)
Theophylline (mM)
0
5
Editing efficiency (%)
n.d
NT
acoC-T2
Cas9
SIBR-Int4 -Cas9
Trends in Biotechnology

and the HArms present on the plasmids. When constitutively expressing Cas9 in combination with the *glcF*-T1 sgRNA, ~10% editing efficiency was observed when the cells were grown in media without theophylline. Including theophylline in the medium resulted in 0% editing efficiency, accompanied also with ~100-fold reduction in total colony counts (Figure 1G and Figure S4). Low editing efficiency (~10%) was also observed when transforming SIBR-Int4-Cas9 combined with *glcF*-T1 sgRNA and plating the transformed cells on noninducing conditions. By contrast, including theophylline in the medium resulted in ~80% editing efficiency, albeit with low total colony counts (Figure 1G and Figure S4). To verify the deletion of *glcEF*, a resulting edited colony was sequenced through Sanger sequencing, confirming the complete deletion of *glcEF* (Figure S6 in the supplemental information online).

To further test the robustness of SIBR-Int4-Cas9 to mediate efficient gene deletion in *C. necator*, we continued by editing the *acoC* locus following the same approach as described for *glcEF* (Figure 1H). Resulting colonies were counted (Figure S4) and screened for the desired edit (Figure S7 in the supplemental information online). Like our *glcEF* knockout assays, NT sgRNA controls showed <5% editing efficiency regardless of the construct or medium used. Using the constitutively expressed Cas9 along with the *acoC*-T2 sgRNA eliminated all the colonies in the presence or absence of theophylline. By contrast, using SIBR-Int4-Cas9 along with the *acoC*-T2 sgRNA resulted in ~95% editing efficiency when the cells were grown on medium containing theophylline (Figure 1I). As observed when editing the *glcEF* locus, high editing efficiency was coupled to a reduced number of total colony counts (Figure S4), suggesting effective counterselection. Complete deletion of *acoC* from an edited colony was also confirmed through Sanger sequencing (Figure S8 in the supplemental information online). Collectively, by controlling the translation of Cas9 in *C. necator* using SIBR-Int4, we demonstrated high (>80%) editing efficiencies at two different genomic loci.

CRISPR-Cas12a is functional in *C. necator*

To further expand the genome editing toolkit available for *C. necator* and to broaden the available target sites in the genome of *C. necator*, we explored whether we can use another Cas protein, Cas12a. This protein has distinct features compared with Cas9, including a different protospacer adjacent motif (PAM) recognition site (5′-(T)TTV-3′) located at the 5′ end of the protospacer sequence, and the ability to process its own crRNA array (due to its RNase activity), which makes it ideal for multiplex genome editing approaches [23,24]. Like our previous tests with Cas9 (Figure 1B,C), we assessed the expression of active CRISPR-Cas12a complexes by constitutively expressing Cas12a (Figure 2A) along with either of two *acoC* targeting (T1 and T2, Table S2) crRNAs or the NT crRNA, followed by plating on selective media and counting the total colony counts (Figure 2B).

Figure 1. Self-splicing Intron-Based Riboswitch (SIBR)-Int4-Cas9 mediates efficient genome editing in *Cupriavidus necator*. (A) Constructs for the constitutive and inducible expression of Cas9 in *C. necator*. The P_{lacUV5} promoter was used for constitutive expression of Cas9 and the single guide (sg)RNA. SIBR (Int2/3/4) was used for the inducible expression of Cas9. Int2/3/4 differ in their 5′ exon sequence. (B) Cas9 targeting assay at the *glcF* locus. The sequences of the *glcF* targeting spacers *glcF*-T1 and *glcF*-T2 are shown. Plasmids expressing either of the targeting (T) sgRNAs or the nontargeting (NT) sgRNA, along with the constitutively expressed Cas9, were introduced through electroporation into *C. necator* and plated on selective solid media. The total colony counts [expressed in colony forming units (CFU)/μg DNA] recovered after each electroporation is shown in (C). The barplots show the average of two electroporation experiments. (D) SIBR-Cas9 targeting assay at the *glcF* locus. Plasmids expressing the *glcF*-T1 or the NT sgRNA, along with the SIBR-Int2/3/4-Cas9, were electroporated into *C. necator*. Transformants were plated on selective solid media with or without theophylline. The total colony counts (expressed in CFU/μg DNA) recovered after each electroporation is shown in (E). The barplots show the average of three electroporation experiments. Editing assays at the *glcEF* (F,G) and *acoC* (H,I) loci. In panels (F) and (H), T (*glcF*-T1, *acoC*-T2) or NT sgRNAs, along with the constitutively expressed Cas9 or the SIBR-Int4-Cas9 were assembled into plasmids which contained homology arms (HArms) to direct recombination at each target locus. Following electroporation, transformed cells were plated on selective solid medium with or without theophylline, the total colony counts (expressed in CFU/μg DNA) was calculated and colony PCR was performed to define the editing efficiency for the *glcEF* deletion (G) and *acoC* deletion (I). Barplots represent the mean of three replicates. For each replicate, up to 16 colonies (or as many as available) were screened through colony PCR. Abbreviations: Kan, kanamycin; LB, lysogeny broth; n.d., not determined.

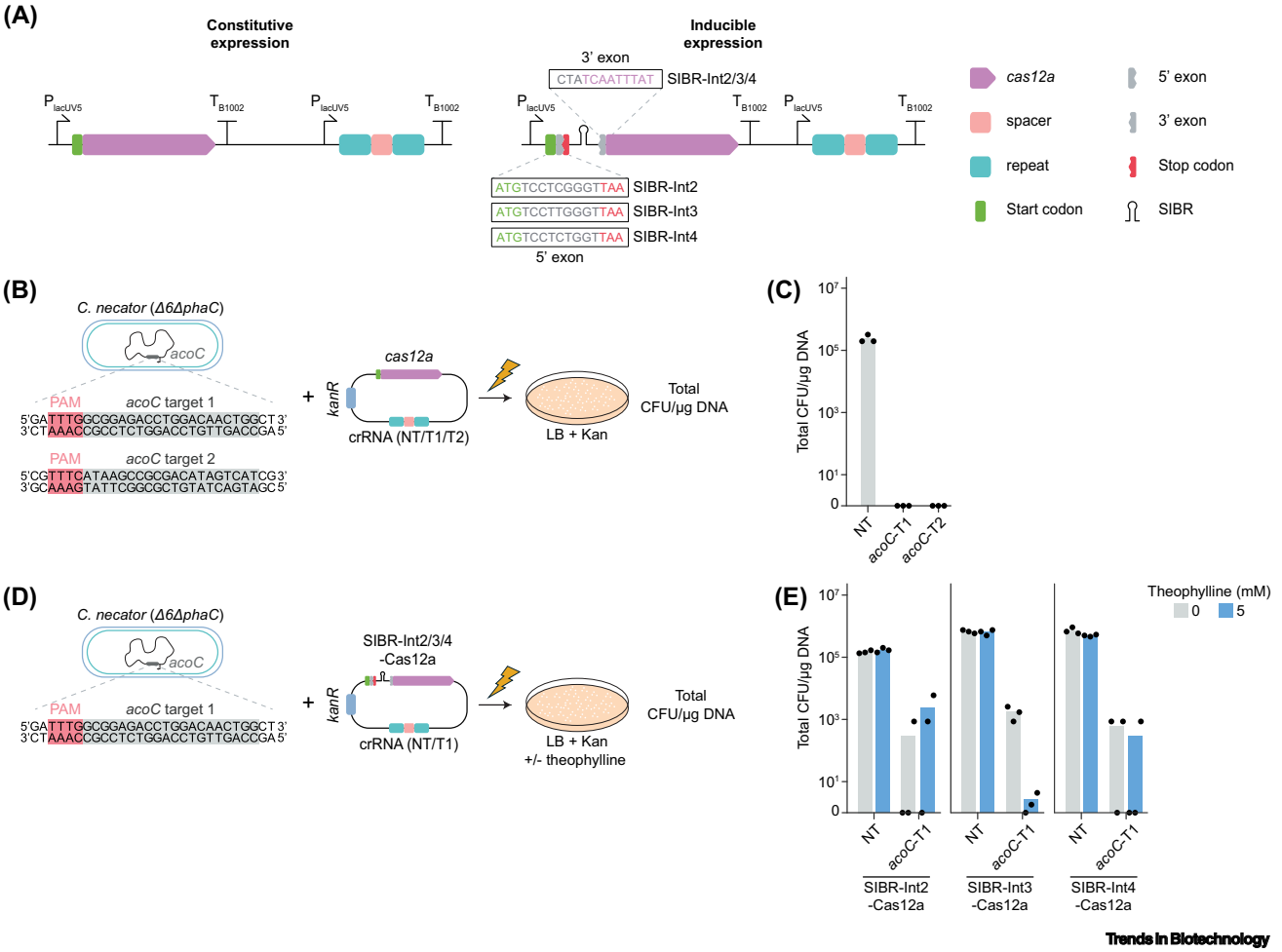

Figure 2. Self-splicing Intron-Based Riboswitch (SIBR) cannot restrict the translation of *cas12a* in *Cupriavidus necator*. (A) Constructs for the constitutive and inducible expression of Cas12a in *C. necator*. The P_{lacUV5} was used for constitutive expression of *cas12a* and the CRISPR (cr)RNA. SIBR (Int2/3/4) was used for the inducible expression of Cas12a. Int2/3/4 differ in their 5′ exon sequence. (B) Cas12a targeting assay at the *acoC* locus. The sequences of the *acoC* targeting spacers *acoC*-T1 and *acoC*-T2 are shown. Plasmids expressing either of the targeting (T) single guide (sg)RNAs or the nontargeting (NT) sgRNA, along with the constitutively expressed Cas12a, were introduced through electroporation into *C. necator* and plated on selective solid media. The total colony counts [expressed in colony forming units (CFU)/μg DNA] recovered after each electroporation is shown in (C). The barplots show the average of three electroporation experiments. (D) SIBR-Cas12a targeting assay at the *acoC* locus. Plasmids expressing the *acoC*-T1 or the NT sgRNA, along with the SIBR-Int2/3/4-Cas12a, were electroporated into *C. necator*. Transformants were plated on selective solid media with or without theophylline. The total colony counts (expressed in CFU/μg DNA) recovered after each electroporation is shown in (E). The barplots show the average of three electroporation experiments. Abbreviations: Kan, kanamycin; LB, lysogeny broth.

For both the *acoC*-T crRNAs, we observed a complete elimination of colonies compared with the NT crRNA control, indicating the functionality of CRISPR-Cas12a for genome targeting in *C. necator* (Figure 2C). As both T crRNAs performed equally well, we selected the *acoC*-T1 crRNA for all subsequent experiments targeting the *acoC* locus.

An alternative translation initiation site within SIBR leads to Cas12a expression

Next, we conducted inducible targeting assays by introducing different variants of the SIBR-Cas12a constructs (Int2, Int3, and Int4) paired with either an NT crRNA or the *acoC*-T1 crRNA, into *C. necator* (Figure 2A,D). Following transformation, cells were selected on solid medium with or without theophylline and the total colony counts were calculated. As expected, NT crRNA controls showed ~10^5 total colony counts in both inducing and noninducing conditions

when either of the three SIBR-Cas12a variants were used. Surprisingly, under noninducing conditions, ~100-fold reduction in total colony counts was observed when the *acoC*-T1 crRNA was combined with either of the three SIBR-Cas12a variants (Figure 2E). This result was unexpected as our previous data on Cas9 showed that SIBR-Int3 and SIBR-Int4 variants did not lead to reduction of total colony counts upon noninducing conditions (Figure 1E). Moreover, as SIBR-Int2-Cas9 did not result in reduced total colony counts even under induction conditions due to its inefficient splicing efficiency, we expected that SIBR-Int2-Cas12a would result in a similar outcome. However, this was not the case as SIBR-Int2-Cas12a resulted in ~100-fold reduction in total colony counts compared with its NT crRNA counterpart, regardless of the presence or absence of the theophylline inducer, indicating towards another mechanism for successful Cas12a expression.

Based on our observations, we hypothesised that there might be two potential causes for the functional expression of Cas12a in all the SIBR-Cas12a variants even in the absence of the theophylline inducer: (i) SIBR is self-splicing out of pre-mRNA transcripts in the absence of theophylline (i.e., leaky self-splicing); or (ii) Cas12a is translated from pre-mRNA transcripts from a secondary ribosome-binding site (RBS) within the intron sequence near the 5′ end of the *cas12a* CDS.

To eliminate the possibility of leakiness due to the self-splicing of SIBR in the absence of theophylline, we introduced a STOP codon within the 5′ exon sequence of SIBR-Cas12a (Figure S9A in the supplemental information online). This design ensures that even if SIBR splices out in the absence of theophylline, a premature STOP codon will preclude the translation of functional Cas12a. As performed previously, plasmids encoding the modified Cas12a expression cassette (paired with either the NT crRNA or the *acoC*-T1 crRNA), were introduced into *C. necator* and cells were plated on solid selective medium. As shown in Figure S9B, the presence of a premature stop codon at the 5′ exon did not eliminate the translation of Cas12a, as a >100 fold reduction in total colony counts was still observed in the absence of the inducer and when the *acoC*-T1 crRNA was used. This result indicated that factors other than leaky self-splicing result in the expression of Cas12a from the encoded pre-mRNA.

Following our second hypothesis, we conducted a bioinformatic analysis of the SIBR-Int4-Cas12a pre-mRNA sequence to identify any alternative RBS from which a functional Cas12a could be fully translated. Using the RBS Calculator biophysical model [25–28], we compared the predicted translation initiation rates (TIR) in *C. necator* over the sequence of both the SIBR-Int4-Cas9 and SIBR-Int4-Cas12a sequences. Although both SIBR-Int4-Cas9 and SIBR-Int4-Cas12a sequences share the same SIBR sequence, they differ in the downstream gene sequence (i.e., the *cas9* and *cas12a* sequence), which can affect the TIR based on the formation of secondary mRNA structures that inhibit the RBS and hinder the translation of the protein.

Interestingly, we identified a translation start site near the 3′ end of the intron sequence where the TIR was predicted to spike for SIBR-Int4-Cas12a, but not for SIBR-Int4-Cas9 (Figure S10 in the supplemental information online). The identified translation start site corresponds to a methionine codon, which is downstream of the final in-frame stop codon of the SIBR sequence and adjacent to the SIBR splicing site. Taken together, this prediction indicates that an alternative RBS site is present in the intron sequence and is recognized by the *C. necator* translation machinery. In the case of SIBR-Cas12a, this results in the full translation of a functional Cas12a that causes cell death when combined with a targeting guide, regardless of the presence or absence of the theophylline inducer. However, as SIBR-Int4-Cas9 is not predicted to have a spike in TIR at the same site as SIBR-Cas12a, Cas9 only gets translated in the presence of theophylline, leading to a tight and inducible protein translation system.

SIBR2.0 – tight and inducible protein expression by transferring the SIBR along the CDS of the target gene

To overcome the apparent limitation encountered when using the original SIBR design to control Cas12a expression in *C. necator* and to broaden the applicability of SIBR for regulating multiple genes across various organisms, we developed an improved version of the SIBR system that we call SIBR2.0. This updated version is not limited to the introduction of SIBR directly after the ATG start codon of the GOI, but it can be introduced along the CDS of the GOI. With SIBR2.0, we achieve two main goals: (i) avoiding the translation of a full-length protein from an alternative RBS site within the SIBR sequence and; (ii) if translation still occurs from the alternative RBS site within the SIBR, this will result in a truncated, nonfunctional protein (Figure S11 in the supplemental information online).

To develop SIBR2.0, SIBR should be installed in the CDS of the GOI at a location that ensures proper intron splicing while maintaining the correct codon sequence after splicing. As the 5′ and 3′ exonic regions adjacent to the intron are known to have a role in intron splicing, any alteration in those regions can result in dysfunctional splicing [29–31]. During our previous study [16], we created a library of T4 *td* introns containing mutations at its 5′ and/or the 3′ flanking exons showing that, although the splicing of the intron is affected by the mutations present at the flanking 5′ or 3′ exons, there is still flexibility in sustaining mutations without detrimental effects to the splicing of the intron. Using this information, we developed a Python script called 'SIBR Site Finder' (see Key Resources Table in the STAR★METHODS online). This script accepts a CDS sequence in FASTA format and returns a CSV file containing the following: (i) a list of the potential SIBR insertion sites along the GOI, (ii) the necessary silent mutations at the SIBR 5′ and 3′ exon sequences that are required for efficient splicing but also for maintaining the correct amino acid sequence after splicing of the SIBR, (iii) the full CDS of the GOI including the alternative SIBR placement, (iv) the amino acid sequence resulting after splicing of the intron, and (v) a score based on the predicted splicing efficiency of the intron (the higher the better). A schematic overview of these algorithmic steps is provided in Figure 3A.

To validate our script and design in a quantitative way, we reasoned that inserting the SIBR at different locations across the CDS of the green fluorescence protein (GFPuv) gene would give us quantitative measurements in a semi high-throughput way. To this end, we chose *E. coli* as a host (the original host where the T4 *td* intron library was generated) and used a plasmid where the *gfpuv* gene is expressed under the P_{tacI} promoter and contains a SIBR in its CDS, at position 29 (SIBR2.0-29-GFPuv), as recommended by the SIBR Site Finder script (see Key Resources Table in the STAR★METHODS online). For controls, we used an empty vector where the *gfpuv* gene was omitted and a plasmid where the *gfpuv* was intact (i.e., no interruption of the gene with the SIBR). To our surprise, we did not observe any measurable fluorescence when the *gfpuv* gene was interrupted with the SIBR and induced with theophylline (Figure S12 in the supplemental information online). To determine whether splicing of the T4 *td* intron is happening at the introduced site, we replaced SIBR with a wild-type T4 *td* intron (i.e., without the theophylline aptamer), introduced it at the exact same site, and repeated our experiment. Similarly, no fluorescence was detected even though the T4 *td* intron should be self-splicing out of the transcript, resulting in a processed mRNA and a fully functional GFPuv protein. Further changing the transcribed gene sequence (*mrfp*), the SIBR insertion position, the promoter (P_{lacUV5}), the induction strength, or even the organism, did not result in any measurable fluorescence (Figure S13 in the supplemental information online).

The absence of fluorescence for all the tested conditions led us to hypothesise that the number of GFPuv (or mRFP) molecules produced after splicing may be insufficient to detect a fluorescent signal using a conventional plate reader. GFP detection is different from our previous successful

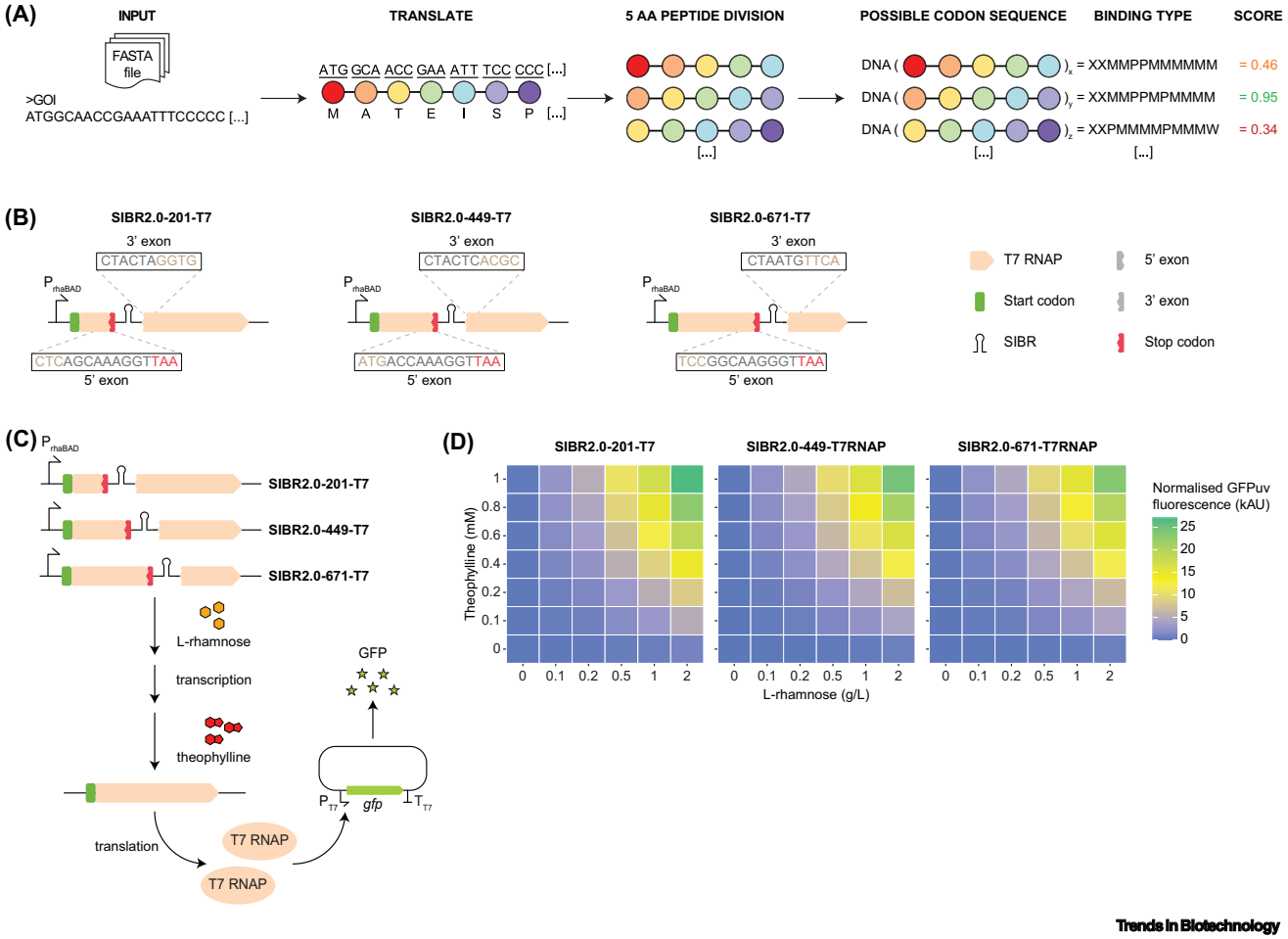

Figure 3. Development of SIBR2.0 in *Escherichia coli*. (A) The 'SIBR Site Finder' algorithm. Implemented in Python, the algorithm takes the coding sequence (CDS) (in FASTA format) of the gene of interest (GOI) as input. First, the DNA sequence is translated. Then, the resulting protein sequence is divided into all possible five amino acid-long peptides. For each peptide, all possible CDSs are computed. Each peptide CDS is then assigned a 'binding type', which codifies the CDS's base pair interactions at the T4 *td* intron P1 stem-loop. The interactions are encoded as follows: X denotes a position where any nucleotide is accepted; P and W indicate Watson–Crick base pairing and wobble base pairing, respectively; M is used to indicate a mismatch. Each binding type is then assigned a score, which measures the predicted splicing efficiency of the intron at each possible insertion site. The top-scoring insertion sites can then be experimentally validated by the user. (B) Insertion of SIBR2.0 along the T7 RNA polymerase (T7 RNAP) CDS. For each SIBR2.0-T7 RNAP construct, the sequence of the 5′ and 3′ intron flanking regions is shown. (C) Signal amplification cascade. Each SIBR2.0-T7 RNAP DNA sequence was placed under the control of the P_{rhaBAD} promoter, creating a dual-level AND gate which controls gene expression at both the transcription and translation level. L-rhamnose and theophylline must both be added to obtain functional T7 RNAP polymerase molecules, which may then mediate the expression of the *gfpuv* gene from the P_{T7} promoter. (D) Output of the signal amplification cascade. For each SIBR2.0-T7 RNAP construct, GFPuv fluorescence was measured across gradients of L-rhamnose and theophylline. For each combination of inducers, the heatmaps show the mean fluorescence of three *E. coli* populations. Abbreviation: SIBR, Self-splicing Intron-Based Riboswitch.

attempts to control the expression of *lacZ* or *cas* genes with SIBR [16], as in those cases the resulting proteins are enzymes that can be measured for their enzymatic activity (LacZ for its multi-turnover β-galactosidase activity and Cas for its genome targeting and cleavage activity resulting in cell death) and not solely by their relative abundance.

We therefore hypothesised that a signal amplification mechanism would be necessary to translate inducible SIBR splicing into detectable GFP fluorescence. To this end, we designed a T7 RNAP - GFPuv cascade system where the SIBR controls the expression of T7 RNAP, a multi-turnover enzyme, which itself can transcribe many molecules of GFPuv under the T7 promoter (Figure 3B,C).

We then used the SIBR Site Finder script and the T7 RNAP CDS as input and chose three insertion sites (between G201 and L202, G449 and L450, and between G671 and L672) to interrupt the T7 *rnap* gene with the SIBR (see Key Resources Table in the STAR★METHODS online). The 5′ and 3′ flanking regions of the SIBR were nearly identical for all three sites and the sites were spread along the T7 RNAP gene to determine the effect of the location of the SIBR (Figure 3B). The three variations of the SIBR2.0-T7RNAP were then integrated into the genome of *E. coli* DH10B (to avoid plasmid copy number variation) and its expression was controlled by the P_{rhaBAD} promoter to attain tight, dual-level control of expression and maximise the signal-to-noise ratio of the cascade system. The three different *E. coli* strains were then tested for their response to both L-rhamnose and theophylline, by measuring end-point fluorescence (Figure 3C,D).

As shown in Figure 3D, all three SIBR insertion sites showed a similar response to L-rhamnose and theophylline addition, suggesting that, at least in this experimental setting and choice of gene, the insertion position of SIBR has little to no effect. In the absence of L-rhamnose, the measured fluorescence was negligible even with the highest tested theophylline concentration (1 mM) for all three variants. Similarly, when the highest concentration of L-rhamnose was used (2 g/l) but the theophylline inducer was omitted, the measured fluorescence was minimal across all three variants, demonstrating the strict nature of the SIBR. Notably, when higher L-rhamnose concentration was used, the fluorescence increased in a linear relation to the corresponding theophylline concentration (Table S3 in the supplemental information online). This linearity demonstrates a tight and tunable expression system, which can be used for various biotechnological applications where tuning of gene expression is desired.

SIBR2.0-Cas12a mediates efficient genome editing in *C. necator*

Having characterised the SIBR2.0 system, we sought to apply it to control Cas12a expression and thereby create a functional system for Cas12a genome editing in *C. necator*. Using the SIBR Site Finder script and the *cas12a* nucleotide sequence as input, we decided to introduce SIBR at amino acid positions 414 and 818 (see Key Resources Table in the STAR★METHODS online), yielding constructs SIBR2.0-414-Cas12a and SIBR2.0-818-Cas12a, respectively (Figure 4A). These positions were selected based on their intron splicing score and their position along the CDS of *cas12a*, ensuring that any alternative translation start site will result in a truncated, nonfunctional protein. The resulting constructs paired with either the *acoC*-T1 crRNA or the NT crRNA were electroporated into *C. necator* cells and were subjected to inducing or noninducing conditions to quantify inducible targeting. SIBR-Int4-Cas12a, which we previously observed to be defective in inducible targeting assays, was used as a control. A reduction in the number of recovered colony counts (>99.9%) was only observed for the SIBR2.0-414-Cas12a and SIBR2.0-818-Cas12a variants when the *acoC*-T1 crRNA was used and when the transformed cells were subjected to inducing conditions (Figure 4B). By contrast, and as previously observed, the SIBR-Int4-Cas12a variant resulted in >100-fold reduction in total colony counts even under uninduced conditions. These results confirm that SIBR2.0 can tightly control Cas12a expression when placed at alternative locations within its CDS and may therefore be used to mediate genome editing in *C. necator*.

Encouraged by our results, we tested whether the SIBR2.0-818-Cas12a plasmid could be used to perform a knockout of the *acoC* gene using an experimental procedure analogous to that described for the SIBR-Int4-Cas9 editing assays. For this purpose, HArms were added to the relevant plasmids and editing assays were performed as described previously and shown in Figure 4C.

For all editing constructs, final editing efficiencies are provided in Figure 4D, and raw data (colony PCR and Sanger sequencing results) are provided in Figures S14 and S15 (see the supplemental

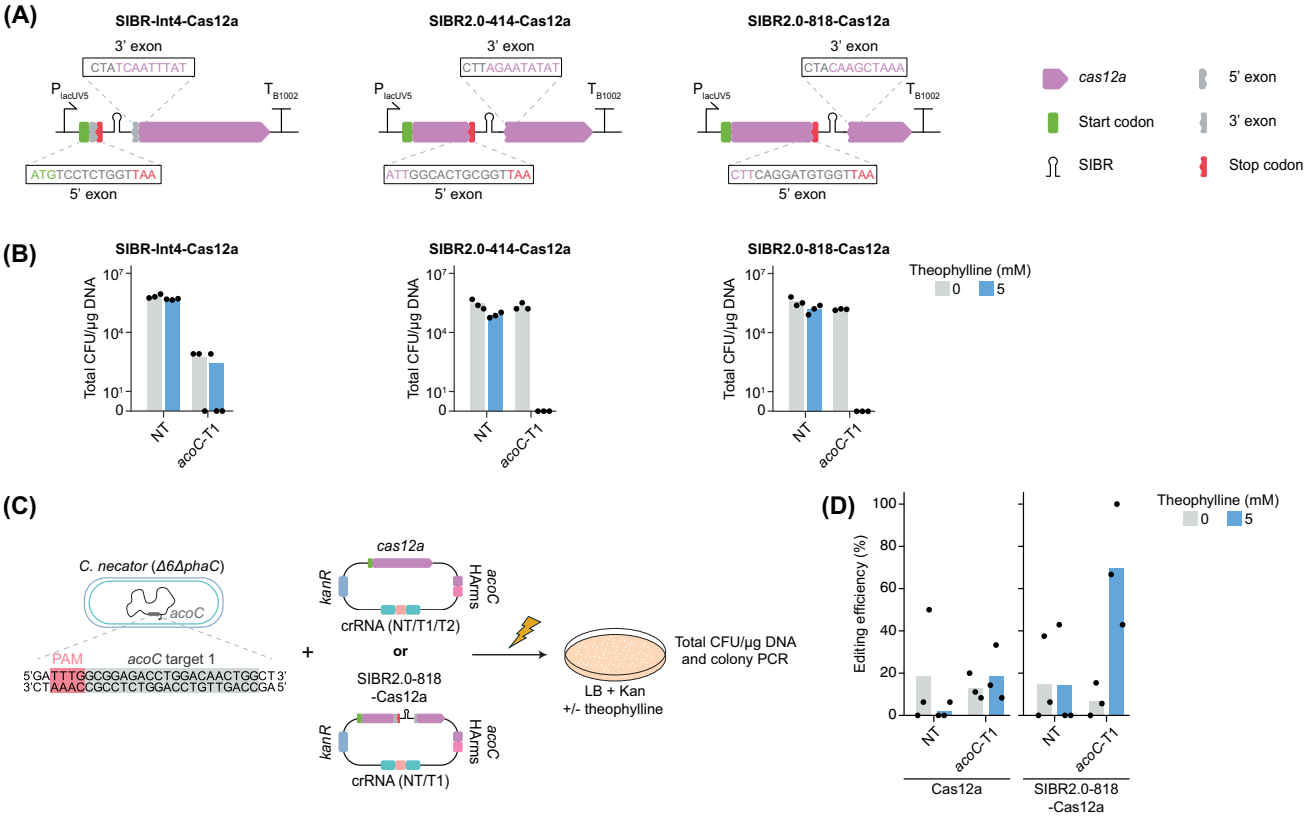

Figure 4. SIBR2.0-Cas12a mediates efficient editing in *Cupriavidus necator*. (A) Self-splicing Intron-Based Riboswitch (SIBR)- and SIBR2.0-Cas12a expression cassettes. The sequence of the 5′ and 3′ intron flanking regions is shown for SIBR-Int4 and the SIBR2.0-Cas12a constructs. (B) Inducible targeting at the *acoC* locus. The expression cassettes shown in (A) were paired with nontargeting (NT) and *acoC*-T1 CRISPR (cr)RNAs to measure inducible targeting efficiency. For each construct and induction condition, barplots show the average number of recovered colonies for three electroporations. (C) Editing assays at the *acoC* gene using SIBR2.0-818-Cas12a. The *acoC*-T1 or the NT crRNAs, along with the constitutively expressed Cas12a or the SIBR2.0-818-Cas12a were assembled into plasmids which contain homology arms (HArms) to direct recombination at the *acoC* target locus. Following electroporation, transformed cells were plated on selective solid medium with or without theophylline, the total colony counts [expressed in colony forming units (CFU)/µg DNA] was calculated, and colony PCR was performed to define the editing efficiency for the *acoC* deletion. (D) Barplots represent the mean of three replicates. For each replicate, up to 16 colonies (as many as available) were screened through colony PCR. Abbreviations: Kan, kanamycin; LB, lysogeny broth.

information online). For the control Cas12a plasmids, low editing efficiency (≤ 20 %) was recorded in all cases and no substantial differences were observed between induced and uninduced conditions. For SIBR2.0-818-Cas12a editing plasmids, a high editing efficiency of ~70% was recorded only when paired with the *acoC*-T1 crRNA under induced conditions. These data demonstrate that counterselection of wild-type genomes by SIBR2.0-Cas12a is necessary and sufficient to mediate highly efficient genome editing in *C. necator*.

Rapid and efficient plasmid curing from *C. necator*

Following genome editing, SIBR plasmids must be removed (cured) from the edited strains to enable iterative editing or transformation of other plasmids. To assess the possibility of curing the SIBR plasmids from *C. necator*, we used the *C. necator* Δ*acoC* strain derived from our editing assays and monitored the loss of its associated SIBR2.0-818-Cas12a editing plasmid. To induce plasmid loss, we subjected the cells to different curing conditions, as previously described [14,32,33]. These involved growing the cells in nonselective lysogeny broth (LB) medium at

30°C with or without rifampicin, or in LB at 37°C without antibiotics. As a control, cells were forced to retain the editing plasmid by culturing in selective LB medium (100 μg/ml kanamycin). We found that culturing edited cells in LB medium without antibiotics at 37°C provided the optimal conditions for plasmid curing, with ≥98% of the cell population becoming sensitive to kanamycin after a single overnight (16 h) incubation (Figure 5A,B). Having demonstrated this final step in the genome editing workflow, we summarise the complete standardised procedure for assembly of SIBR-Int4-Cas9 and SIBR2.0-818-Cas12a editing plasmids (Figure 5C) and subsequent iterative genome editing in *C. necator* (Figure 5D).

Discussion

In this work, we focused on expanding and improving the genome editing toolbox of *C. necator*, a promising microbial platform for CO_2 valorisation [7,34,35]. To this end, we developed several advances that simplify the genome editing pipeline and enhance the genome editing efficiency in *C. necator*.

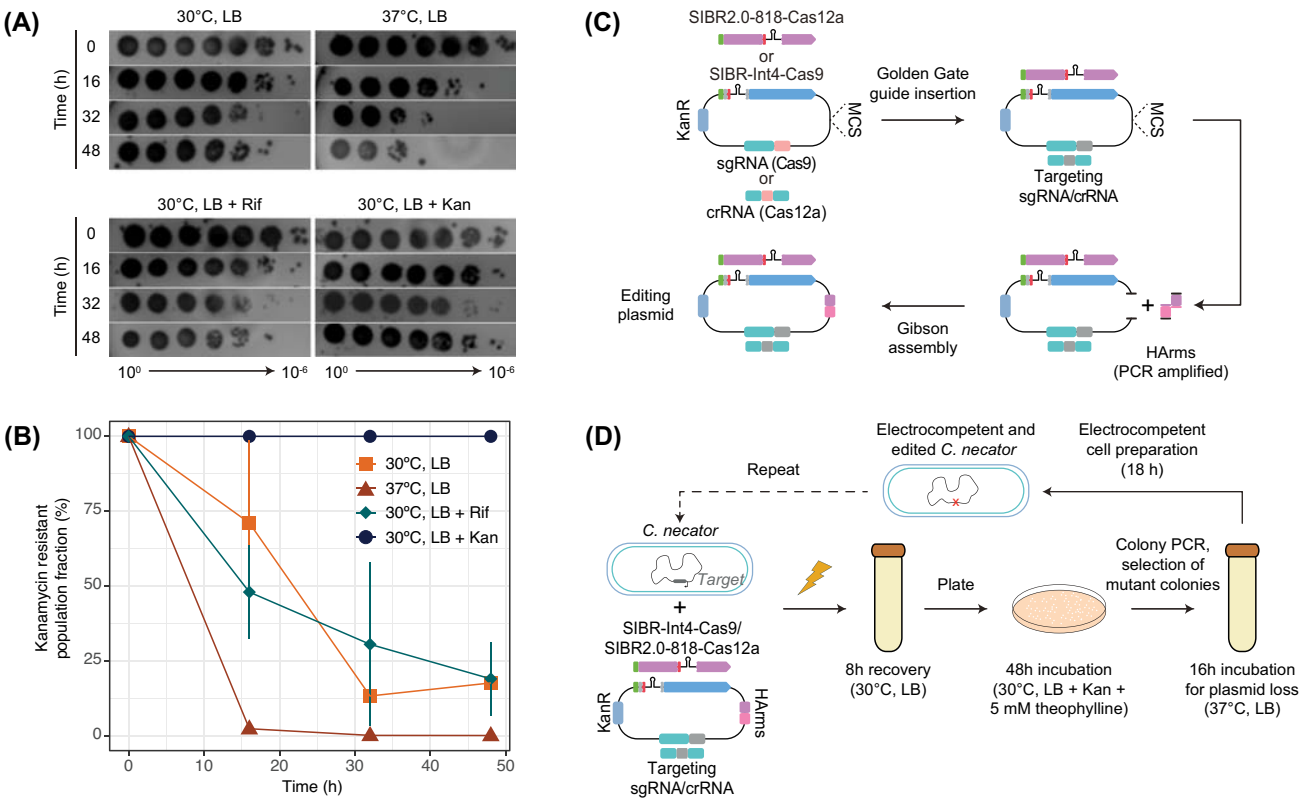

Figure 5. Workflow for Self-splicing Intron-Based Riboswitch (SIBR)-based genome editing of *Cupriavidus necator*. (A) Monitoring the loss of SIBR plasmids in populations of edited cells. Representative serial dilutions of cultures on selective agar plates [lysogeny broth (LB) with 100 μg/ml kanamycin] at the time of each passage. For each dilution time series, the plasmid curing condition is indicated. Colony counts from each deletion series were used to quantify the kanamycin-resistant fraction of each bacterial population, as shown in (B). Individual points indicate the average of $n = 3$ replicates ± one standard deviation. (C) Assembly of SIBR-Int4-Cas9 and SIBR2.0-818-Cas12a editing plasmids. Using the features of the standardised SIBR plasmid backbones, single guide (sg)RNA or CRISPR (cr) RNA spacers can be inserted onto the plasmids via Golden Gate assembly. The assembly products can then be used directly for insertion of the homology arms (Harms). The plasmid backbone is linearised using one of the restriction sites present within the Multiple Cloning Site (MCS). HArms, which have been previously PCR-amplified from genomic DNA, are then assembled with the linearised backbone via Gibson assembly. (D) Workflow for (iterative) genome editing. SIBR-Int4-Cas9 or SIBR2.0-818-Cas12a editing plasmids are electroporated into *C. necator*. Transformants are plated onto selective solid medium and the resulting colonies are screened for editing at the target locus. Confirmed deletion mutants can then be cured of the editing plasmids via overnight incubation in LB medium at 37°C, enabling iterative editing or introduction of alternative plasmids.

First, we implemented a novel electroporation protocol that enabled rapid transformation of the large (~7–9 kb) SIBR plasmids with high efficiency. Though it is difficult to compare the performance of the electroporation protocol across existing publications that use plasmids of different sizes and use different properties to measure transformation efficiency [14,33,36,37], by using the *C. necator* Δ*H16_A0006* strain we obtained transformation efficiencies of up to ~10^5–10^7 total colony counts with large, unmodified plasmids isolated from *E. coli*. This streamlined and efficient protocol reduced the hands-on time and streamlined both targeting and editing assays to a total of ~48 h.

Second, we adapted the original SIBR design [16] and used it to tightly and inducibly control the expression of the Cas9 protein in *C. necator*, resulting in >80% editing efficiency when targeting the *glcEF* or *acoC* genes. The high editing efficiency achieved by SIBR-Int4-Cas9 matches or outcompetes other existing genome editing approaches in *C. necator* [14,15], although at a faster turnaround time of ~48 h after electroporation with the editing plasmid.

Third, we developed SIBR2.0 that widens the applicability of the SIBR system. This development arises through our observation that, in our plasmid context, the original SIBR-Cas design could not repress the expression of Cas12a in *C. necator*. Through a series of experiments, we discovered that an alternative translation initiation site exists within SIBR, is recognised by the *C. necator* translation machinery, and leads to the complete and functional translation of Cas12a. The alternative translation initiation site appears to be gene- and/or organism-specific as the original SIBR design was sufficient to control Cas9 but not Cas12a expression in *C. necator* and was sufficient to control Cas12a expression in *E. coli* [16]. To overcome this limitation and to create a more versatile SIBR system, we developed SIBR2.0, which includes the introduction of SIBR at a more central position in the CDS of the GOI. This advancement ensures that even in the presence of an alternative initiation site, the translated protein will be truncated and therefore nonfunctional. We then used SIBR2.0 to tightly and inducibly control Cas12a expression in *C. necator*, resulting in ~70% editing efficiency when targeting the *acoC* gene. To our knowledge, this is the first successful use of CRISPR-Cas12a to edit the genome of *C. necator*, further expanding the genome editing toolbox in this species.

Fourth, we showed that by following our novel setup, it is possible to generate a knockout *C. necator* strain within ~48 h after electroporation and have a plasmid-free strain ready for downstream applications or iterative editing within ~4 days. This timeline represents at least a 50% reduction compared with the time required for generating a mutant as reported by previous studies [14]. Our reduced protocol is even more streamlined relative to traditional suicide-vector systems (i.e., pLO3), where generating a clean mutation takes usually 10–12 days [9]. Moreover, using the SIBR system, we achieved gene knockout efficiencies ranging between 70% and 80%, which are comparable with the editing efficiencies reported by previous studies [14].

Last, during the development of SIBR2.0, we also developed the SIBR Site Finder script that allows the user to find appropriate sites along the CDS of the GOI to introduce SIBR2.0. We demonstrated the functionality of the script by introducing SIBR2.0 in multiple sites along the CDS of the GOI as demonstrated in the T7 RNAP-GFPuv (sites 201, 449, or 671) and Cas12a (sites 414 or 818) assays, without an observable reduction in GFPuv fluorescence or targeting efficiency, respectively, at any of the introduction sites. We also showed that SIBR2.0 is a tight gene expression system as demonstrated by our T7 RNAP-GFPuv assay

which included a dual control system (rhamnose inducible promoter and SIBR2.0). Tight control using SIBR2.0 was also demonstrated during our Cas12a targeting assays as cell death was only observed when using a targeting guide RNA and when theophylline was included in the medium.

Overall, in this study we expanded the genome editing toolbox and streamlined genome editing in *C. necator* by developing both SIBR-Int4-Cas9 and SIBR2.0-818-Cas12a systems. We anticipate that these innovations will enable the rapid and iterative generation of engineered *C. necator* strains (gene knockouts and gene insertions) and will facilitate the translation of this species into a robust microbial cell factory. Furthermore, due to its tight and versatile nature, we expect that SIBR2.0 will open a new frontier for the tight and inducible expression of toxic proteins, the use of SIBR2.0 in genetic logic gates and genetic circuits, and the use of SIBR2.0-Cas for genome editing in microbes characterised by low endogenous HR efficiency.

Concluding remarks

Simple, efficient, and rapid genome editing tools are desirable features to accelerate the transition from laboratory-scale to industrial-scale biotechnological applications. To date, many genome editing tools are confined to well-described model organisms, whereas non-model organisms are confined to inefficient and laborious genome editing tools. One such non-model organism, *C. necator*, was used in our study to demonstrate the development of a streamlined genome editing toolkit, by using the SIBR-Cas system. Through a stepwise approach, we show that SIBR can be used to tightly and inducibly control CRISPR-Cas9 counterselection, leading to high editing efficiencies in *C. necator*. Moreover, we developed SIBR2.0, which is an updated version of SIBR that can be used to control the expression of virtually any protein of interest in the target organism. We used SIBR2.0 to control the Cas12a protein in *C. necator* and achieved high knockout efficiencies of the target gene.

Due to the simplicity of SIBR and SIBR2.0 (introduced after the start codon or within the CDS as recommended by the SIBR Site Finder script, respectively), the use of the theophylline inducer for splicing of SIBR that can readily permeate the membrane of both Gram-positive and Gram-negative bacteria, and the absence of any additional exogenous factors (e.g., expression of recombinases), we anticipate that the SIBR and SIBR2.0 systems will be used by the community of microbiologists and cell engineers. Applications may include the tight and temporal control of CRISPR-Cas (or any other genome editors, e.g., IscB, TnpB, Argonautes) for efficient genome editing, or to control the expression of any GOI in the target microbe.

Overall, this study developed two simple, efficient, and rapid genome editing tools for editing the genome of the industrially relevant microbe *C. necator* H16. Although our tool showed robustness across different genes and different microorganisms, there are still several challenges that must be addressed (see Outstanding questions), before achieving the full potential of our tool.

STAR★METHODS

Detailed methods are provided in the online version of this paper and include the following:

- KEY RESOURCES TABLE
- EXPERIMENTAL MODEL AND STUDY PARTICIPANT DETAILS
- METHOD DETAILS
  - Electroporation of *C. necator*
  - Theophylline toxicity assay
  - Assembly of SIBR-Cas9 plasmids
  - Assembly of SIBR-Cas12a and SIBR2.0-Cas12a plasmids
  - CRISPR-Cas targeting and editing assays

Outstanding questions

How can we enhance the endogenous homologous recombination efficiency and avoid the toxic effect of CRISPR-Cas counterselection?

Can SIBR and SIBR2.0 be used efficiently to control the expression of toxic proteins (other than Cas proteins)?

What is the percentage of spliced pre-mRNA molecules upon SIBR induction with theophylline and how can we increase the splicing efficiency?

Can we exchange the theophylline aptamer of SIBR with another aptamer that: (i) binds a nontoxic inducer compound that maintains the SIBR splicing efficiency; (ii) the inducer compound has good and universal bacterial cell permeability; (iii) the inducer compound cannot be metabolised by the organism of interest?

Can SIBR and SIBR2.0 maintain their splicing efficiency and functionality in extremophiles (e.g., psychrophiles, thermophiles)?

Can other group I, II, or III introns (other than the T4 *td* intron) be repurposed into SIBRs?

- Curing of pSIBR plasmids
- Construction of *E. coli* SIBR-T7 RNAP strains
- GFPuv fluorescence measurements
- Flow cytometry for single time point fluorescence measurements

- QUANTIFICATION AND STATISTICAL ANALYSIS

RESOURCE AVAILABILITY

Lead contact

Requests for further information and resources should be directed to and will be fulfilled by the lead contact, Constantinos Patinios (constantinos.patinios@gmc.vu.lt).

Materials availability

pCas9-NT (Addgene plasmid # 235165), pSIBR-Int4-Cas9-NT (Addgene plasmid # 235166), pCas12a-NT (Addgene plasmid # 235167), and pSIBR2.0-818-Cas12a-NT (Addgene plasmid # 235168) have been deposited to Addgene.

Data and code availability

All raw data used for main text and supplementary figures can be found in Document S1 in the supplemental information online. The softwares generated in this study (SIBR Spacer Designer and SIBR Site Finder) are available on GitHub (https://github.com/sdellavalle/SIBR_spacer_design and https://github.com/sdellavalle/SIBR_Site_Finder) and Google Colab (https://colab.research.google.com/drive/1YPr9gsQCorReDJ8bLyKJLoIuPtBzai6c?usp=sharing and https://colab.research.google.com/drive/162gIZKXOs_sCmV0ZcGzc57ZvEu7QULyA?usp=sharing) (see Key Resources Table). Any additional information will be made available from the lead contact upon reasonable request.

Author contributions

Conceptualization: S.D.V., E.O., S.C.A.C., R.H.J.S., J.v.d.O, C.P., methodology: S.D.V., E.O., S.C.A.C., C.P., *C. necator* targeting and editing assays: S.D.V., E.O., L.F.M.J., E.N.P., *E. coli* assays: S.C.A.C., script writing: S.D.V., S.C.A.C., Script depositing: S.D.V., H.S., writing manuscript: S.D.V., E.O., C.P., reviewing and editing manuscript: all authors, figure generation: S.D.V., E.O., C.P., supervision: C.L.B., H.S., N.J.C., P.I.N., R.H.J.S., J.v.d.O, W.E.H., C.P., funding acquisition: E.O., C.L.B., R.H.J.S., J.v.d.O, P.I.N., W.E.H.

Acknowledgments

We would like to express our gratitude to Dr Belén Adiego-Pérez and Rob Joosten for their technical assistance in this project. Moreover, we would like to thank Evans Asamoah Gyimah for his help towards the development of SIBR2.0. S.D.V and W.E.H thank the EPSRC & BBSRC Centre for Doctoral Training in Synthetic Biology (EP/L016494/1), and EPSRC (EP/M002403/1 and EP/N009746/1). E.O. is supported by the European Union's Horizon 2020 Research and Innovation Program under the Marie Skłodowska-Curie grant agreement no. 101065339 (ROAD). H.S. is supported in part by the EPSRC project EP/W000326/1. P.I.N. acknowledges funding from the Novo Nordisk Foundation (NNF10CC1016517, NNF20CC0035580, and NNF18CC0033664). R.H.J.S. is supported by the Dutch Research Council (NWO VIDI grant VI.Vidi.203.074). N.J.C is supported by the Dutch Research Council (NWO Veni grant VI.Veni.192.156). J.v.d.O acknowledges the Dutch Research Council (NWO Spinoza grant SPI 93-537 and NWO Gravitation grant 024.003.019), and the European Research Council (ERC-AdG-834279) for financial support. C.P. acknowledges funding from the Research Council of Lithuania under the Programme University Excellence Initiatives of the Ministry of Education, Science and Sports of the Republic of Lithuania (Measure No. 12-001-01-01-01, Improving the Research and Study Environment), project No: S-A-UEI-23-10.

Declaration of interests

C.P., S.C.A.C, J.v.d.O., and R.H.J.S are inventors of a patent related to the technology developed in this study (WO2022074113). C.L.B. is a cofounder and officer of Leopard Biosciences, cofounder and scientific advisor to Locus Biosciences, and scientific advisor to Benson Hill. J.v.d.O. and R.H.J.S. are shareholders and members of the scientific board of Scope Biosciences B.V., and J.v.d.O. is a scientific advisor of NTrans Technologies and Hudson River Biotechnology. The other authors have no conflicts of interest to declare.

Supplemental information

Supplemental information associated with this file can be found online https://doi.org/10.1016/j.tibtech.2025.02.006.

References

1. Liu, Z. *et al.* (2020) Third-generation biorefineries as the means to produce fuels and chemicals from CO2. *Nat. Catal.* 3, 274–288
2. Della Valle, S. *et al.* (2024) Construction of microbial platform chassis for CO2 utilisation. *Curr. Opin. Syst. Biol.* 37, 100489
3. Humphreys, C.M. and Minton, N.P. (2018) Advances in metabolic engineering in the microbial production of fuels and chemicals from C1 gas. *Curr. Opin. Biotechnol.* 50, 174–181
4. Volke, D.C. *et al.* (2023) Emergent CRISPR-Cas-based technologies for engineering non-model bacteria. *Curr. Opin. Microbiol.* 75, 102353
5. Panich, J. *et al.* (2021) Metabolic engineering of *Cupriavidus necator* H16 for sustainable biofuels from CO2. *Trends Biotechnol.* 39, 412–424
6. Li, H. *et al.* (2012) Integrated electromicrobial conversion of CO2 to higher alcohols. *Science* 335, 1596
7. Pan, H. *et al.* (2021) Synthetic biology toolkit for engineering *Cupriviadus necator* H16 as a platform for CO2 valorization. *Biotechnol. Biofuels* 14, 212
8. Lenz, O. *et al.* (1994) The *Alcaligenes eutrophus* H16 hoxX gene participates in hydrogenase regulation. *J. Bacteriol.* 176, 4385–4393
9. Lenz, O. and Friedrich, B. (1998) A novel multicomponent regulatory system mediates H2 sensing in *Alcaligenes eutrophus*. *Proc. Natl. Acad. Sci. U. S. A.* 95, 12474–12479
10. Peoples, O.P. and Sinskey, A.J. (1989) Poly-beta-hydroxybutyrate (PHB) biosynthesis in *Alcaligenes eutrophus* H16. Identification and characterization of the PHB polymerase gene (phbC). *J. Biol. Chem.* 264, 15298–15303
11. Srivastava, S. *et al.* (1982) Mutagenesis of *Alcaligenes eutrophus* by insertion of the drug-resistance transposon Tn5. *Arch. Microbiol.* 131, 203–207
12. Dronsella, B. *et al.* (2022) Engineered synthetic one-carbon fixation exceeds yield of the Calvin cycle. *bioRxiv*, Published online October 20, 2022. https://doi.org/10.1101/2022.10.19.512895
13. Park, J.M. *et al.* (2010) Development of a gene knockout system for *Ralstonia eutropha* H16 based on the broad-host-range vector expressing a mobile group II intron. *FEMS Microbiol. Lett.* 309, 193–200
14. Xiong, B. *et al.* (2018) Genome editing of *Ralstonia eutropha* using an electroporation-based CRISPR-Cas9 technique. *Biotechnol. Biofuels* 11, 172
15. Collas, F. *et al.* (2023) Engineering the biological conversion of formate into crotonate in *Cupriavidus necator*. *Metab. Eng.* 79, 49–65
16. Patinios, C. *et al.* (2021) Streamlined CRISPR genome engineering in wild-type bacteria using SIBR-Cas. *Nucleic Acids Res.* 49, 11392–11404
17. Dykstra, J.C. *et al.* (2022) Metabolic engineering of *Clostridium autoethanogenum* for ethyl acetate production from CO. *Microb. Cell Factories* 21, 243
18. Claassens, N.J. *et al.* (2020) Phosphoglycolate salvage in a chemolithoautotroph using the Calvin cycle. *Proc. Natl. Acad. Sci. U. S. A.* 117, 22452–22461
19. Priefert, H. *et al.* (1991) Identification and molecular characterization of the *Alcaligenes eutrophus* H16 aco operon genes involved in acetoin catabolism. *J. Bacteriol.* 173, 4056–4071
20. Jugder, B.-E. *et al.* (2015) An analysis of the changes in soluble hydrogenase and global gene expression in *Cupriavidus necator* (*Ralstonia eutropha*) H16 grown in heterotrophic diauxic batch culture. *Microb. Cell Factories* 14, 42
21. Windhorst, C. and Gescher, J. (2019) Efficient biochemical production of acetoin from carbon dioxide using *Cupriavidus necator* H16. *Biotechnol. Biofuels* 12, 163
22. Bommareddy, R.R. *et al.* (2020) A sustainable chemicals manufacturing paradigm using CO2 and renewable H2. *iScience* 23, 101218
23. Zetsche, B. *et al.* (2015) Cpf1 is a single RNA-guided endonuclease of a class 2 CRISPR-Cas system. *Cell* 163, 759–771
24. Patinios, C. *et al.* (2023) Multiplex genome engineering in *Clostridium beijerinckii* NCIMB 8052 using CRISPR-Cas12a. *Sci. Rep.* 13, 10153
25. Salis, H.M. *et al.* (2009) Automated design of synthetic ribosome binding sites to control protein expression. *Nat. Biotechnol.* 27, 946–950
26. Espah Borujeni, A. *et al.* (2017) Precise quantification of translation inhibition by mRNA structures that overlap with the ribosomal footprint in N-terminal coding sequences. *Nucleic Acids Res.* 45, 5437–5448
27. Espah Borujeni, A. *et al.* (2014) Translation rate is controlled by coupled trade-offs between site accessibility, selective RNA unfolding and sliding at upstream standby sites. *Nucleic Acids Res.* 42, 2646–2659
28. Reis, A.C. and Salis, H.M. (2020) An automated model test system for systematic development and improvement of gene expression models. *ACS Synth. Biol.* 9, 3145–3156
29. Pichler, A. and Schroeder, R. (2002) Folding problems of the 5' splice site containing the P1 stem of the group I thymidylate synthase intron: substrate binding inhibition in vitro and mis-splicing in vivo. *J. Biol. Chem.* 277, 17987–17993
30. Chu, F.K. *et al.* (1984) Intervening sequence in the thymidylate synthase gene of bacteriophage T4. *Proc. Natl. Acad. Sci. U. S. A.* 81, 3049–3053
31. Chu, F.K. *et al.* (1986) Characterization of the intron in the phage T4 thymidylate synthase gene and evidence for its self-excision from the primary transcript. *Cell* 45, 157–166
32. Boy, C. *et al.* (2022) Study of plasmid-based expression level heterogeneity under plasmid-curing like conditions in *Cupriavidus necator*. *J. Biotechnol.* 345, 17–29
33. Azubuike, C.C. *et al.* (2021) pCAT vectors overcome inefficient electroporation of *Cupriavidus necator* H16. *New Biotechnol.* 65, 20–30
34. Davison, P.A. *et al.* (2022) Engineering a rhodopsin-based photo-electrosynthetic system in bacteria for CO2 fixation. *ACS Synth. Biol.* 11, 3805–3816
35. Tu, W. *et al.* (2023) Engineering artificial photosynthesis based on rhodopsin for CO2 fixation. *Nat. Commun.* 14, 8012
36. Tee, K.L. *et al.* (2017) An efficient transformation method for the bioplastic-producing "knallgas" bacterium *Ralstonia eutropha* H16. *Biotechnol. J.* 12, 11
37. Vajente, M. *et al.* (2024) Using *Cupriavidus necator* H16 to provide a roadmap for increasing electroporation efficiency in nonmodel bacteria. *ACS Synth. Biol.*, Published online October 31, 2024. https://doi.org/10.1021/acssynbio.4c00380
38. Ehsaan, M. *et al.* (2021) The pMTL70000 modular, plasmid vector series for strain engineering in *Cupriavidus necator* H16. *J. Microbiol. Methods* 189, 106323
39. Huang, W. and Wilks, A. (2017) A rapid seamless method for gene knockout in *Pseudomonas aeruginosa*. *BMC Microbiol.* 17, 199
40. Wenk, S. *et al.* (2020) An "energy-auxotroph" *Escherichia coli* provides an in vivo platform for assessing NADH regeneration systems. *Biotechnol. Bioeng.* 117, 3422–3434
41. Mougiakos, I. *et al.* (2019) Efficient Cas9-based genome editing of *Rhodobacter sphaeroides* for metabolic engineering. *Microb. Cell Factories* 18, 204
42. Hanko, E.K.R. *et al.* (2020) A genome-wide approach for identification and characterisation of metabolite-inducible systems. *Nat. Commun.* 11, 1213

STAR★METHODS

KEY RESOURCES TABLE

Reagent or resource	Source	Identifier
Chemicals, peptides, and recombinant proteins		
Lysogeny Broth (LB)	Sigma-Aldrich	L3522
Super Optimal Broth (SOB)	Sigma-Aldrich	H8032
M9 Minimal Salts 5X	Sigma-Aldrich	M6030
Theophylline	Sigma-Aldrich	T1633
DreamTaq® DNA polymerase	ThermoFisher Scientific	EP0703
Esp3I	New England BioLabs	R0734S
AscI	New England BioLabs	R0558S
BbsI-HF®	New England BioLabs	R3539S
PaqCI ®	New England BioLabs	R0745S
Critical commercial assays		
Monarch® Spin Plasmid Miniprep Kit	New England BioLabs	T1110S
NEBuilder® HiFi DNA Assembly Master Mix	New England BioLabs	E2621S
DNA Clean & Concentrator-5 Kit	Zymo Research	D4004
Bacterial and virus strains		
Escherichia coli DH5α	ThermoFisher Scientific	N/A
Escherichia coli DH10B T1	ThermoFisher Scientific	N/A
Cupriavidus necator H16 *ΔH16_A0006ΔphaC*	Arren Bar-Even Lab	N/A
Oligonucleotides		
Table S2 in the supplemental information online	This paper	N/A
Recombinant DNA		
Table S1 in the supplemental information online	This paper	N/A
Software and algorithms		
R and RStudio (v4.1.2)	RStudio Software	https://posit.co/download/rstudio-desktop/
Python (v3.11.8)	Python software	https://www.python.org/downloads/
FlowJo (v9)	BD Biosciences	https://www.flowjo.com
SIBR Spacer Designer (Python software)	This paper	https://github.com/sdellavalle/SIBR_spacer_design
SIBR Spacer Designer (Google Colab notebook)	This paper	https://colab.research.google.com/drive/1YPr9gsQCorReDJ8bLyKJLoIuPtBzai6c?usp=sharing
SIBR Site Finder (Python software)	This paper	https://github.com/sdellavalle/SIBR_Site_Finder
SIBR Site Finder (Google Colab notebook)	This paper	https://colab.research.google.com/drive/162gIZKXOs_sCmV0ZcGzc57ZvEu7QULyA?usp=sharing
Other		
UV-1800 UV/Vis spectrophotometer	Shimadzu	Item #EW-83400-20
Bio-Rad MicroPulser Electroporator	Bio-Rad Laboratories	1652100
96-well transparent flat bottom microplate	Greiner Bio-One	650101
96-well Masterblock® Polypropylene 2ml microplate	Greiner Bio-One	780270
96-well black clear bottom microplate	Perkin-Elmer	6005182
Spark® multimode microplate reader	Tecan	N/A

(continued on next page)

(continued)

Reagent or resource	Source	Identifier
Synergy MX multimode microplate reader	Biotek	N/A
Sorvall Legend Centrifuge	ThermoFisher Scientific	75004532
BD FACSCalibur flow cytometer	BD Biosciences	N/A

EXPERIMENTAL MODEL AND STUDY PARTICIPANT DETAILS

All bacterial strains used in this study are listed in the Key Resources Table. Plasmid and linear DNA used in this study are listed in Table S1. Additionally, raw data for all the experiments can be found in Document S1 (see the supplemental information online).

Strain *C. necator* H16 Δ*H16_A0006ΔphaC* was obtained as a gift from Dr Arren Bar-Even's lab and was chosen because it harbours a deletion that enhances the strain's electroporation efficiency [14,38]. Unless otherwise stated, plasmids were cloned and propagated in, and isolated from, *E. coli* DH5α. Electroporation of *E. coli* strains was performed as previously described [16]. Plasmids were purified using the NEB Monarch® Miniprep Kit according to the manufacturer's specifications. For routine cultivations of both *E. coli* and *C. necator*, bacteria were grown in liquid Lysogeny Broth (LB) (10 g/l tryptone, 5 g/l yeast extract, 10 g/l sodium chloride) or in Super Optimal Broth (SOB) (20 g/l tryptone, 5 g/l yeast extract, 0.5 g/l sodium chloride, 0.186 g/l potassium chloride, 100 μM magnesium chloride), or on solid LB medium (15 g/l agar). Where relevant, bacteria were grown in M9 mineral medium (50 mM Na_2HPO_4, 20 mM KH_2PO_4, 1 mM NaCl, 20 mM NH_4Cl, 2 mM $MgSO_4$ and 100 μM $CaCl_2$, pH 7.2), supplemented with trace elements (134 μM EDTA, 13 μM $FeCl_3{\cdot}6H_2O$, 6.2 μM $ZnCl_2$, 0.76 μM $CuCl_2{\cdot}2H_2O$, 0.42 μM $CoCl_2{\cdot}2H_2O$, 1.62 μM H_3BO_3, 0.081 μM $MnCl_2{\cdot}$4H2O) and the appropriate carbon source, as specified. *E. coli* cultures were incubated at 37°C and shaking orbitally at 200 rpm. *C. necator* strains were grown at 30°C with shaking orbitally at 150 rpm. Bacterial optical density (600 nm) was measured using a UV-1800 UV/Vis spectrophotometer (Shimadzu). Where appropriate, antibiotics were added at the specified concentrations: kanamycin (*E. coli*: 50 μg/ml, *C. necator*: 100 μg/ml), ampicillin (*E. coli*: 100 μg/ml), chloramphenicol (*E. coli*: 35 μg/ml), and rifampicin (*C. necator*: 50 μg/ml).

METHOD DETAILS

Electroporation of *C. necator*

Electrocompetent *C. necator* cells were prepared using a novel protocol, adapted from an existing method used for *Pseudomonas aeruginosa* [39]. Bacterial strains were streaked out from glycerol stocks onto LB agar plates and incubated for 48 h at 30°C. Bacterial cultures in 5 mL SOB medium were then inoculated from single colonies and incubated overnight (16-18 h). A small volume (~200 μl) of the saturated overnight cultures was used to inoculate larger 50 mL cultures in SOB medium, in 250 mL conical flasks, which were grown to an OD_{600} of 5. Following incubation, 50 mL liquid cultures were split into two 50 mL tubes (25 ml each) and pelleted by centrifugation at 4000 rpm for 10 min at room temperature. All subsequent steps in electrocompetent cell preparation and electroporation were also performed using room-temperature equipment and reagents. Cell pellets were washed twice in 1 mM $MgSO_4$. Each cell pellet was then resuspended in 1 ml 1 mM $MgSO_4$. Cells were pooled, and sterile 50%(v/v) glycerol was added to a final concentration of ~25%(v/v). Cells were divided into 50 μl aliquots in 1.5 ml microcentrifuge tubes and frozen at -80°C. For transformation, competent cell aliquots were thawed and mixed with plasmid DNA (250 ng). Electroporation was performed using 0.2 cm gap electroporation cuvettes, at 2.5 kV, using default setting Ec2 in a Bio-Rad MicroPulser electroporator (Bio-Rad Laboratories). Immediately after electroporation, 0.95 ml of recovery medium (SOB) was added. The resulting 1 ml of culture was transferred to a 1.5 ml microcentrifuge tube and incubated at 30°C with 150 rpm shaking for 2 h (recovery), unless otherwise specified. Following recovery, cells were serially diluted and plated onto selective LB plates to enable quantification of transformation efficiency or resulting colony forming units (CFU) per μg of DNA.

Theophylline toxicity assay

Theophylline toxicity in *C. necator* was quantified via a minimum inhibitory concentration assay at the microplate scale. Cells were cultured overnight (16-18 h) in LB medium (5 ml cultures in 50 ml conical centrifuge tubes). Cells from saturated overnight cultures were pelleted by centrifugation, spent medium was discarded, and the cell pellet was resuspended in fresh LB medium, adjusting the cell density to an OD_{600} of 1. Cells were used to inoculate fresh cultures in a transparent 96-well microplate (Greiner Bio-One)

by diluting them 1:10 into the plate wells, giving a starting OD_{600} = 0.1. The total volume of each well was 150 µl and covered with 50 µl of sterile mineral oil (Sigma-Aldrich) to prevent evaporation. Theophylline was added to microplate wells by diluting a 40 mM stock solution to give working concentrations in the range of 0-20 mM, as indicated. The microplate was incubated at 30°C with double orbital shaking in a Spark microplate reader (Tecan), with OD_{600} measurements taken at 15 min intervals over a period of 24 has described before [40].

Assembly of SIBR-Cas9 plasmids

The Cas9 endonuclease used in this work was obtained from the codon-harmonised *Streptococcus pyogenes* (*Spcas9*) sequence previously developed for *Rhodobacter sphaeroides* [41]. To generate the SIBR-Cas9 plasmid series, the *Spcas9* sequence was cloned via HiFi Assembly (New England Biolabs) in an expression cassette under the control of the lacUV5 promoter (P_{lacUV5}) and the B1002 terminator. The P_{lacUV5} and the B1002 terminator were part of the original SIBR-Cas architecture and were maintained in our constructs for simplified cloning purposes. Similarly, the sgRNA construct from the *R. sphaeroides* CRISPR-Cas9 plasmid was also cloned within a second expression cassette which is also controlled by P_{lacUV5} and B1002 terminator. The different SIBR introns were subsequently cloned after the start codon of *cas9* using Gibson Assembly.

Design of the sgRNAs for CRISPR-Cas9 targeting was performed using the custom "SIBR Spacer Designer" Python software (*see* Key Resources Table for details). The sgRNA spacers were ordered as complementary single-stranded DNA (ssDNA) oligonucleotides (IDT). All sgRNA and crRNA spacer sequences are summarised in Table S2. Forward and reverse oligonucleotides were mixed in equimolar amounts and annealed by incubating the mixture at 95°C for 5 min in 20 mM NaCl solution, followed by cooling at room temperature (22°C) for 2 h. The annealed double-stranded oligonucleotides were assembled into the relevant plasmids via Golden-Gate using PaqCI (NEB), as described previously [16]. Introduction of the homology arms (HArms) required the linearization of the plasmids with AscI (NEB) followed by Gibson Assembly with the amplified HArms.

Correct plasmid assembly was confirmed via Sanger sequencing (Eurofins Genomics) or Nanopore sequencing (Plasmidsaurus Inc).

Assembly of SIBR-Cas12a and SIBR2.0-Cas12a plasmids

SIBR-Cas12a plasmids (pSIBR002, pSIBR003, pSIBR004, pSIBR005) [16] were used to assemble all the SIBR plasmids in this study. We modified the NT spacer sequence from the default sequence present on these plasmids, to ensure compatibility with *C. necator*. The "SIBR Spacer Designer" custom Python software was used to design the crRNA spacer sequences for each target locus, as described for the SIBR-Cas9 sgRNAs (see Key Resources Table). The final sequences (Table S2) were synthesised as oligonucleotides (IDT) and annealed as described above for SIBR-Cas9 with the exception that the BbsI enzyme (NEB) was used for Golden-Gate assembly.

The SIBR2.0 constructs were assembled by PCR amplification of the SIBR sequence and the SIBR plasmid backbones from pSIBR001 and pSIBR005, respectively. Amplicons were assembled by Gibson Assembly, inserting SIBR at the target positions along the *cas12a* CDS, as recommended by the "SIBR Site Finder" Python script (see Key Resources Table). Gibson assembly of HArms into the SIBR2.0-Cas12a editing plasmids was performed as described above for SIBR-Cas9 constructs, with the exception that enzyme Esp3I (NEB) was used for linearization of the plasmid backbone.

Correct assembly was confirmed via Sanger sequencing (Eurofins Genomics) or Nanopore sequencing (Plasmidsaurus Inc).

CRISPR-Cas targeting and editing assays

To measure the targeting efficiency of CRISPR-Cas9 and CRISPR-Cas12a complexes in *C. necator*, the resulting colony forming units (CFU) per µg of DNA were quantified after transforming *C. necator* electrocompetent cells with plasmids encoding nontargeting (NT) or targeting (T) guides. Electrocompetent cells were prepared and transformed following the protocol outlined above. For constitutive targeting assays, the total colony counts were quantified via spot microdilution on selective LB agar plates (100 µg/ml kanamycin). For inducible targeting assays, dilutions were also performed on selective plates with 5 mM theophylline. For editing assays, the recovery step in the electroporation protocol was extended to 8 h, whilst the volume was kept constant at 1 ml. For each plasmid and condition, editing efficiency was quantified by colony PCR (cPCR) using DreamTaq® DNA polymerase (ThermoFisher Scientific), following the standard protocol. A maximum of 16 colonies (or as many as available) were analysed for each replicate, plasmid, and

condition. For all assays, transformation plates were incubated at 30°C for 48 h before single colonies could be counted and genotyped by cPCR, as required.

Curing of pSIBR plasmids

To cure SIBR-Cas plasmids after genome editing, single colonies corresponding to deletion mutants were collected and cultured at 30°C overnight in 5 ml selective LB medium (100 μg/ml kanamycin). Cells from these pre-cultures were used to inoculate test cultures for each curing condition in 5 ml of the appropriate medium, as indicated, in 50 ml conical centrifuge tubes. A 1:100 dilution was used for inoculation, leading to a starting OD_{600} of ~0.02. Cells were grown to saturation in each test condition and serially passaged every 16 h by diluting the cultures 1:100. At each passage, the total number of cells in the culture was quantified by spotting serial dilutions on nonselective LB solid medium. Plasmid-bearing (kanamycin-resistant) cells were analogously quantified on selective plates (solid LB medium with 100 μg/ml kanamycin). Test conditions for plasmid curing were (i) LB medium, 30°C, 150 rpm, (ii) LB medium, 37°C, 150 rpm, or (ii) LB medium, 50 μg/ml rifampicin, 150 rpm. Additionally, cultures in selective LB medium (100 μg/ml kanamycin) at 30°C and 150 rpm shaking were used for the duration of the assays as negative controls for plasmid loss (i.e., to provide a baseline measurement for plasmid retention).

Construction of *E. coli* SIBR-T7 RNAP strains

E. coli DH10B cells (Invitrogen; C640003) harbouring the pSC020 plasmid were made electrocompetent as described previously [16], while being induced with 10 mM L-arabinose (for λRed expression). Next, the P_{rhaBAD}-SIBR2.0–201/449/671-T7 *rnap-lox* cassettes were amplified and contained 5′ (47 nt) and 3′ (49 nt) overhangs to allow for the integration of the P_{rhaBAD}-SIBR2.0–201/449/671-T7 *rnap-lox* cassette between the *ybh*B and the *ybh*C genes, in the genome of *E. coli* DH10B. The cassettes were then purified with a DNA Clean & Concentrator-5 kit (Zymo Research) and introduced into electrocompetent *E. coli* DH10B harbouring pSC020 and recovered for 2.5 h at 30°C. The bacteria were then plated on solid LB medium containing 100 mg/l ampicillin (selecting for pSC020) and 35 mg/l chloramphenicol (selecting for integration of the cassettes) and incubated at 30°C for 16 h. Resulting colonies were cultured in 5 ml LB medium containing 1 mM IPTG and incubated at 30°C for 7 h to allow Cre recombination and removal of the chloramphenicol resistance gene. Then, the cultures were incubated at 37°C in LB medium for 16 h to cure the pSC020 plasmid. Cultures were then streaked on LB solid medium and grown at 37°C for 16 h. Single colonies were tested by PCR for the integration of the cassettes and the removal of the chloramphenicol resistance gene. The amplified fragments were also sequenced with Sanger sequencing to ensure intact integration of the cassettes. Also, the colonies were streaked on LB solid medium containing 100 mg/l ampicillin to ensure the loss of pSC020.

GFPuv fluorescence measurements

The *E. coli* DH10B P_{rhaBAD}-SIBR2.0–201/449/671-T7 *rnap* strains were transformed through electroporation with the GFPuv reporter plasmid pSC028 and selected on selective (50 mg/l kanamycin) solid LB medium. Resulting colonies were grown for 16 h at 37°C in 5 ml selective (50 mg/l kanamycin) LB medium. A 96-well 2-ml culture plate (Greiner Bio-One) was filled with a concentrate of theophylline and L-rhamnose and was diluted with LB medium containing kanamycin and overnight grown bacteria to reach a final kanamycin concentration of 50 mg/l, a final bacterial dilution of 10^{-3} and a theophylline and L-rhamnose concentration which varied between 0 and 1 mM and 0 and 2 g/l, respectively, creating a combinatorial screen of all possible induction conditions across the plate wells.

Culture plates were incubated at 37°C for 16 h shaking orbitally at 200 rpm. Then, the bacteria were centrifuged for 10 min at 4800 g in a Sorvall Legend centrifuge. The supernatant was discarded, and the cell pellet was resuspended in 500 μl 50 mM Tris-HCl (pH 7.5) buffer. After resuspension, the plates were incubated at 37°C for 1 h to allow maturation of the GFPuv. 100 μl of the suspension was pipetted into a 96-well black plate with clear bottom (Perkin Elmer) and measured with a Synergy MX plate reader (Biotek). The cell density was measured by absorbance at 600 nm and the fluorescence was measured at an excitation wavelength of 395 nm with a width of 20 nm and an emission wavelength of 508 nm with 20 nm width with a gain of 50. The background fluorescence and background scattering were subtracted, and the fluorescence was divided by the scattering at 600 nm.

Flow cytometry for single time point fluorescence measurements

Fluorescence measurements were performed to quantify the gene expression output of P_{lacUV5}in *C. necator*. The protocol for single time-point fluorescence measurements was adapted from [42]. Strains carrying test and control plasmids were cultured overnight

(16 h) in selective LB medium (100 μg/ml kanamycin). All cultures used in these experiments had a total volume of 5 mL and cultured in 50 ml conical centrifuge tubes. Overnight cultures were used to inoculate fresh cultures in selective M9 mineral medium, with 20 mM fructose as sole carbon source, at a starting OD_{600} = 0.05-0.1. Cells were grown to mid-exponential phase (OD_{600} = 0.3-0.6), at which point 1 ml of each culture was transferred to 1.5 ml microcentrifuge tubes. Cells were pelleted by centrifugation and washed twice in phosphate buffered saline solution (PBS, 10 mM phosphate buffer, 3 mM KCl, pH 7.4). After the final wash, cell pellets were resuspended in 1 ml PBS, then diluted in PBS to an OD_{600} = 0.01. The cells were analysed using a BD FACSCalibur flow cytometer (BD Biosciences). mRFP fluorescence was measured with a 488 nm laser and a 585/42 nm emission band-pass filter (corresponding to the instrument's FL2 channel). The voltage of the FL2 detector was set to 705 V and the amplitude gain was adjusted to 1.0. At least 100 000 events were collected for each sample. Flow cytometry data was analysed using the proprietary FlowJo software (BD Biosciences).

QUANTIFICATION AND STATISTICAL ANALYSIS

Data analysis and visualisation was carried out using Microsoft Excel 365 and RStudio. To ensure reproducibility, all experiments were carried out with independent biological replicates. For each experimental data set reported in this study, the number of independent replicates is detailed in the relevant figure legends, together with a description of the summary statistics that are shown (mean, standard deviation, confidence interval, as appropriate). Raw data for all experiments can be accessed in the supplemental information online (Document S1 in the supplemental information online).